

A SELF-SEPARATION ALGORITHM USING SPEED CONTROL FOR WIDTH-LIMITED HIGH DENSITY AIR CORRIDOR

Yoichi NAKAMURA*, Noboru TAKEICHI**, Keisuke FUKUOKA**

*Air Traffic Management Department, Electronic Navigation Research Institute

**Department of Aerospace Engineering, Nagoya University

Keywords: *Air Traffic Management, Self-Separation, Air Corridor*

Abstract

Algorithms for self-separation of aircraft operating in a high density air corridor are discussed. An air corridor is a tube or band-shaped piece of airspace that connects high-demand city areas etc. Aircraft in the air corridor all fly in the same direction, and only aircraft capable of self-separation may operate in the air corridor. An appropriate self-separation algorithm is indispensable to realizing high traffic throughput while maintaining safety. In this paper, an algorithm for self-separation of aircraft in a width-limited band-shaped piece of airspace has been developed. The algorithm refers to the relative position and speed of aircraft for conflict avoidance based on the assumption that all aircraft intend to fly along the air corridor. It is demonstrated that all the aircraft are able to self-separate without conflict in the width-limited air corridor. It is also demonstrated that self-separation using current state information results in a deadlock in the narrow air corridor. As the corridor width increases, aircraft utilize more space to overtake and aircraft are able to fly at their optimum speed. Additionally, it is indicated that the installation of sub-route and utilization of optimum speed information prevent a deadlock even though the corridor width is narrow.

1 Introduction

To accommodate future air traffic demand while maintaining safety, a higher Air Traffic Management (ATM) system capability is

required along with advanced communication, navigation, and surveillance technologies. The air corridor is an operational concept proposed in the NextGen (Next Generation Air Transportation System) [1], and CARATS (Collaborative Actions for Renovation of Air Traffic Systems) [2] programs to increase ATM capacity. The air corridor is generally considered as a long and narrow tube or band-shaped piece of airspace connecting high demand area. In the corridor, only aircraft capable of self-separation are allowed to fly in the same direction, and aircraft are self-separated without ATC (air traffic control) instructions. The self-separation is technically enabled by use of Automatic Dependent Surveillance Broadcast (ADS-B) [3]. Under ADS-B, aircraft periodically broadcast its own position, altitude, velocity vector, etc. Therefore, aircraft are able to monitor the surrounding aircraft and self-separate from them. Since the corridor is segregated from conventional airspace, ATC provides instructions only to the aircraft outside of the corridor. Being free from workload constraint associated with ATC, an implementation of air corridor operations are expected to improve both the safety and capacity in the whole airspace. Since the self-separation potentially reduces separation standard, aircraft are expected to fly closer to their optimum route, which results in the improvement of efficiency.

To implement the corridor operations, some safe and efficient operational procedures are indispensable. The air corridor concept including the corridors' geometry and allocation

have been studied[4-6]. However the detail of self-separation procedures has not been studied prior to the authors' ones[7-11]. The authors have studied to clarify the feasibility of the operation of the self-separation. A self-separation algorithm through heading change for one-way high density traffic flow [7] and a route structures for the safer and more efficient traffic flow [8] have been investigated. Additionally, a basic self-separation algorithm for air corridor operation based on the assumption that all aircraft fly in the same direction has been proposed [9-11]. However, the corridor width limitation has not yet been strictly considered. In this paper, the algorithm for width-limited air corridor is investigated. This paper demonstrated the behavior of the aircraft in a high density air corridor through numerical simulations.

2 Simulation Model

2.1 Traffic Flow Model

In this study, only the level motion of aircraft is considered. For conflict detection and resolution, a minimum separation distance and a separation control distance are introduced. As shown in Fig. 1, the minimum separation distance is denoted by a circle centered at aircraft with radius R_{MS} , and the separation control distance is denoted by a dashed circle with radius R_{SC} . Aircraft perform the conflict detection and resolution referring to the separation control distance R_{SC} .

As a traffic density increases, it is considered difficult to realize the safe and efficient traffic flow. A procedure that can accommodate maximum density traffic is also capable of common density traffic. Hence, this study focuses on algorithms that accommodate the maximum traffic volume. The maximum volume is defined as the volume of traffic where all aircraft form a row with the distance equal to the separation control distance as shown in Fig. 2.

In this paper, a simple straight width-limited corridor is considered and all aircraft fly in the same direction at their optimum flight speed as shown in Fig. 3. Self-separation

algorithms are investigated through numerical simulations of the air corridor with the maximum volume.

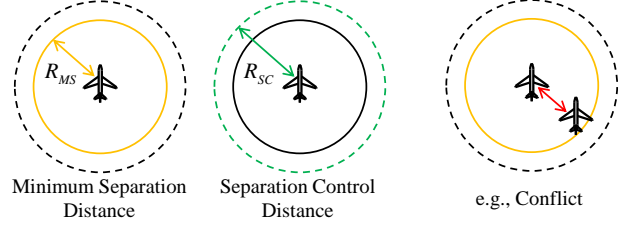


Figure 1. Minimum separation distance and separation control distance.

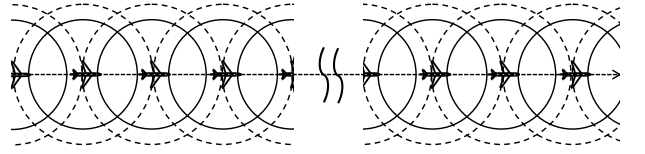


Figure 2. Traffic flow with maximum volume

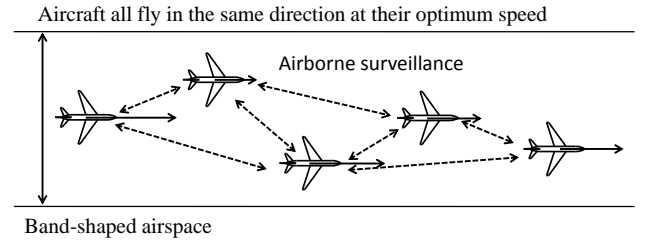


Figure 3. Traffic flow in the air corridor.

2.2 Equation of Motion

The aircraft is modeled as a mass particle, and the coordinate system is shown in Fig. 4. The x axis is defined as the direction parallel to the corridor. The y axis is perpendicular to the x axis. The equations of motion are given as follows:

$$\dot{x}_i = V_i \cos \psi_i \quad (1)$$

$$\dot{y}_i = V_i \sin \psi_i \quad (2)$$

$$\dot{V}_i = a_i \quad (3)$$

$$\dot{\psi}_i = \frac{g \tan \phi_i}{V_i} \quad (4)$$

Where V , a , ψ , and ϕ represent the aircraft velocity, acceleration, heading angle, and bank angle, respectively. i denotes the aircraft number and g is the gravitational acceleration.

The acceleration and bank angle are given as follows:

$$\varphi_i = \alpha_1(\Psi_i - \psi_i) \quad (5)$$

$$a_i = \alpha_2(V_{ii} - V_i) \quad (6)$$

Where Ψ_i and V_{ii} represent the target heading angle and speed, α_1 and α_2 are parameters. The target values are determined in accordance with surrounding aircraft, which is described in the following section.

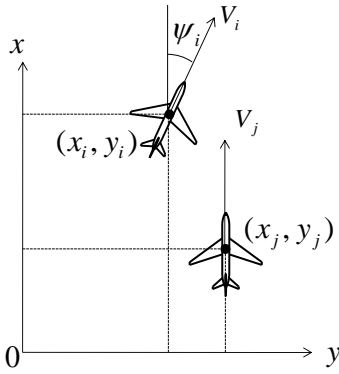


Fig. 4. Coordinate system

2.3 Self-Separation Algorithm

The self-separation algorithm has been developed based on the assumption that all aircraft fly in the same direction [10]. Consider the aircraft A overtaking the aircraft B shown as case 1 in Fig. 5, where dy_{AB} is the distances between these aircraft along the y axis. When dy_{AB} is less than R_{SC} and V_B is less than V_A , aircraft should perform maneuvers for conflict resolution. In this study, it is assumed that the faster aircraft turns the heading to the right, and the slower one does the heading to the left because the algorithm that determines the turning direction based on their relative speed achieves a drastic improvement in control amount while maintaining safety in high density air corridor [11]. On the other hand, in the situation shown as case 2 in Fig. 5, aircraft B should not turn the heading to the left to prevent conflict with aircraft C. In this case, only aircraft A change their heading to avoid conflict. To determine their maneuver, the limitations of heading angle are introduced. Aircraft determine their maneuver referring the limitations to complete overtaking process without conflict with surrounding aircraft.

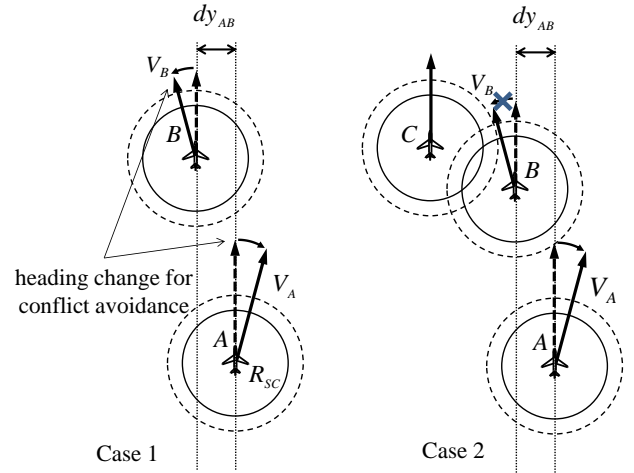


Fig. 5. Example of maneuver for conflict avoidance

The heading angles to determine their maneuver are obtained based on the relative position and speed. Firstly, the heading angle for conflict avoidance is described considering the aircraft A overtaking the aircraft B shown in Fig. 6, where dx_{AB} is the distances between these aircraft along the x axis. To maintain the distance larger than the R_{SC} , aircraft A changes its heading by μ so that the velocity vector V_R directed along the line tangential to the circle as shown Fig. 6. The heading angle μ is obtained from the following equations:

$$\frac{dy_{AB}^{ip}}{V_A \sin \mu} = \frac{dx_{AB}^{ip}}{V_A \cos \mu - V_B} \quad (7)$$

$$\mu = \sin^{-1} \left(\frac{dy_{AB}^{ip}}{\sqrt{dy_{AB}^{ip\ 2} + dx_{AB}^{ip\ 2}}} \right) - \sin^{-1} \left(\frac{dx_{AB}^{ip}}{\sqrt{dy_{AB}^{ip\ 2} + dx_{AB}^{ip\ 2}}} \frac{V_B}{V_A} \right) \quad (8)$$

where dx_{AB}^{ip} is the distance between aircraft A and tangent point along the x axis, and dy_{AB}^{ip} is the one along the y axis as shown in Fig. 6. These equations mean the time for the aircraft A to reach the separation control circle of the aircraft B along the tangential line.

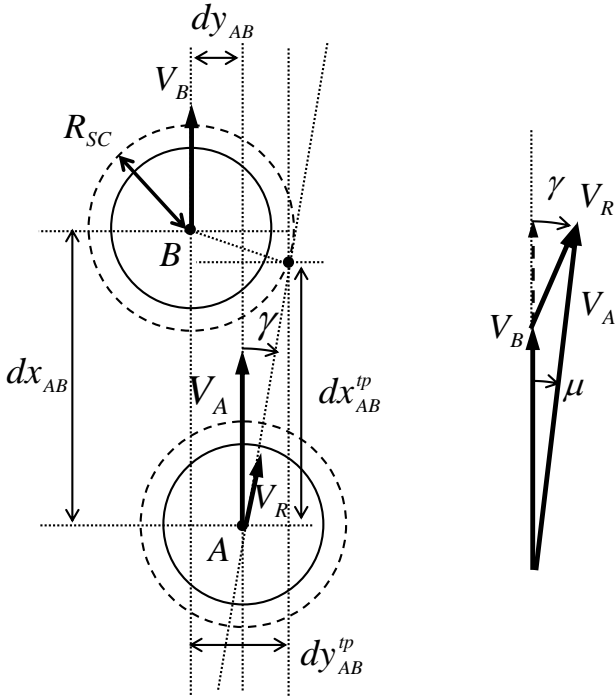


Fig. 6. Heading angle for conflict avoidance

Secondly, the limitations of heading angle are described. Since aircraft need to move along the y axis up to R_{SC} when aircraft overtake another aircraft ahead of them, overtaking should be performed within a scope which does not affect other surrounding aircraft. In the situation shown in Fig. 7, rightward maneuver of aircraft A to overtake another aircraft might result in the conflict with aircraft C. In this study, heading angle limit is introduced to avoid conflict. The upper limit of heading angle H_{ulim} that aircraft A could change without approach within the circle centered at aircraft C with radius R_{SC} is obtained as following equation as the same way above:

$$\frac{dy_{AC}^{ulp}}{V_A \sin \mu} = \frac{dx_{AC}^{ulp}}{V_A \cos \mu - V_C} \quad (9)$$

$$\mu = \sin^{-1} \left(\frac{dy_{AC}^{ulp}}{\sqrt{dy_{AC}^{ulp2} + dx_{AC}^{ulp2}}} \right) - \sin^{-1} \left(\frac{dx_{AC}^{ulp}}{\sqrt{dy_{AC}^{ulp2} + dx_{AC}^{ulp2}}} \frac{V_C}{V_A} \right) \quad (10)$$

while aircraft A changes its heading under H_{ulim} , conflict with aircraft C is not expected. If multiple aircraft are in the surveillance range,

upper limit of heading angle is calculated for each aircraft, and the maximum value is assumed as H_{ulim} .

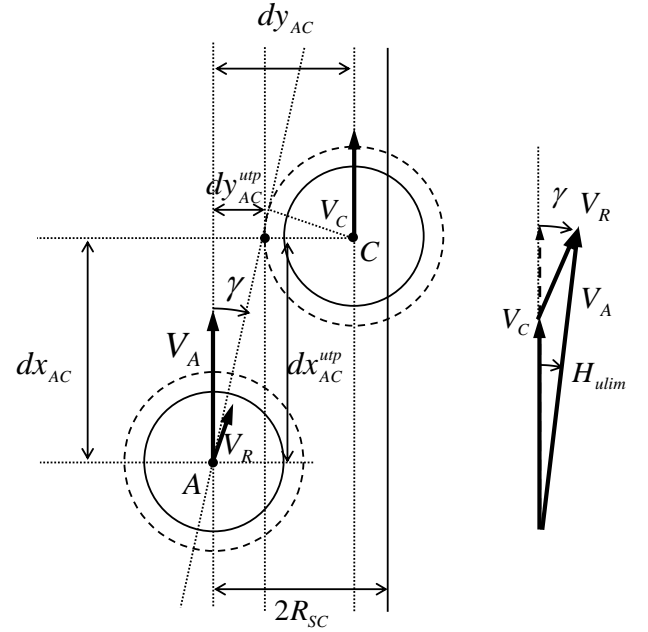


Fig. 7. Upper limit of heading angle

The lower limit of heading angle H_{olim} is also introduced. Consider the same situation as above shown in Fig. 8. When the heading angle of aircraft A is larger than H_{olim} , aircraft A could maintain sufficient distance to aircraft C. H_{olim} is derived as the same way as H_{ulim} .

$$\frac{dy_{AC}^{olp}}{V_A \sin H_{olim}} = \frac{dx_{AC}^{olp}}{V_A \cos H_{olim} - V_C} \quad (11)$$

$$\mu = \sin^{-1} \left(\frac{dy_{AC}^{olp}}{\sqrt{dy_{AC}^{olp2} + dx_{AC}^{olp2}}} \right) - \sin^{-1} \left(\frac{dx_{AC}^{olp}}{\sqrt{dy_{AC}^{olp2} + dx_{AC}^{olp2}}} \frac{V_C}{V_A} \right) \quad (12)$$

while aircraft A changes its heading over H_{olim} , conflict with aircraft C is not expected. If multiple aircraft are in the surveillance range, lower limit of heading angle is calculated for each aircraft, and the minimum value is assumed as H_{olim} .

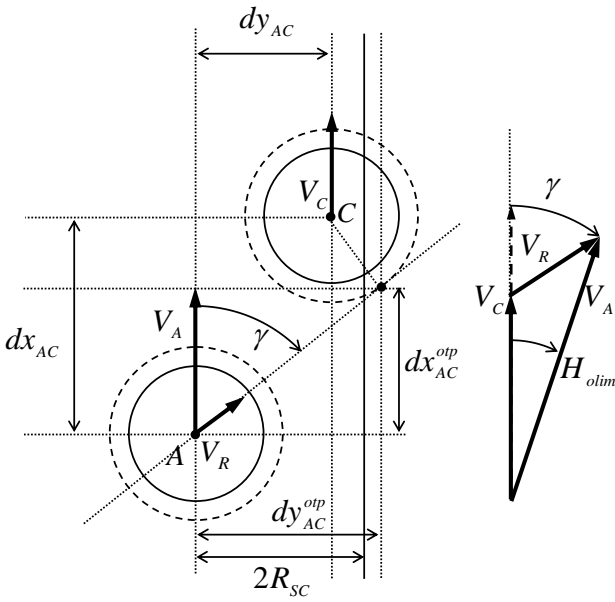


Fig.8. Lower limit of heading angle

Furthermore, another upper limit of heading angle is also introduced to achieve safe air traffic flow within the air corridor. Previous study demonstrated the large heading change result in the conflict [9] and almost all aircraft could self-separate from each other within a range of heading change by 10 degrees [11]. Therefore, in this study, the upper limit of angle is defined as the function of the distance from the corridor edge which has the maximum value of 10 degrees as shown Fig. 9. H_w is expressed as follows:

$$H_w = \min(10, \alpha_3(dy_{edge} - y_i)) \quad (13)$$

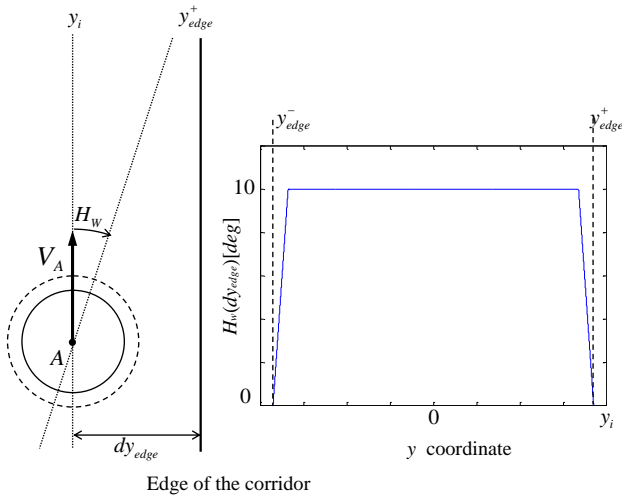


Fig.9. Upper limit of heading angle for prevention of deviation from air corridor

In this study, all the aircraft change their heading within H_w . Aircraft determine the maneuver comparing the limitations of heading angles. Conditions where aircraft perform overtaking using heading change are as follows;

$$H_{olim} \leq \mu \leq H_w \quad (14)$$

$$\mu \leq \min(H_{olim}, H_w) \quad (15)$$

when heading angle required to avoid conflict is in the range of above equations, aircraft change their heading by as large angle as possible to avoid another aircraft. Otherwise, it is expected that aircraft are not able to avoid conflict by means of heading change. In this case, aircraft maintain the distance using speed control. Aircraft change their speed to the average speed of the approaching aircraft as follows;

$$V_{it} = \frac{\sum_{k=1}^N V_k}{N} \quad (16)$$

where N is the number of approaching aircraft within a range of lateral distance of R_{SC} . The following aircraft reduce their speed and the preceding aircraft increase their speed. In case the distance becomes shorter than R_{MS} , aircraft change their speed as the same speed as the preceding aircraft.

The self-separation algorithm is summarized as follows. When conflict is detected, aircraft try to avoid by means of heading change within the limitations so that aircraft do not deviate the corridor. Only when aircraft cannot avoid by heading change, aircraft maintain the distance by means of speed control.

3 Numerical Simulations

3.1 Simulation Parameters

Characteristics of traffic flow in the air corridor are examined through numerical simulations. Since the traffic flow in the corridor is considered to be affected by the width of the corridor, air corridors with different width (10, 20, 30NM) are considered. Table. 1 summarizes the simulation parameters and Fig. 10 depicts a

display example of aircraft in the corridor, where the circle centered at aircraft has radius R_{SC} . To identify the traffic behavior and to eliminate the influence of the initial conditions, long term simulations are necessary. Hence, the air corridor model shown in Fig. 10 is used, where the right and left edges are assumed to be linked and aircraft on the right edge monitor the ones on the left edge, and vice versa. The length of corridor is 100 NM, and air traffic flow is composed of 20 aircraft. The behavior of aircraft for 100,000 s is computed. The aircraft are placed along x axis with intervals equal to the separation control distance, and randomly along y axis for the initial condition. The optimum flight speed for each aircraft is uniformly distributed between 450 kt to 500 kt. The minimum separation distance R_{MS} and the separation control distance R_{SC} are set 3 NM and 5 NM, respectively. Numerical simulations are carried out using 30 set of initial conditions.

Table. 1 Simulation parameters

# of aircraft	20
Speed range	450-500 kt
RMS	3 NM
RSC	5 NM
α_1	1
α_2	10^{-2} 1/s
α_3	10^{-4} rad/m

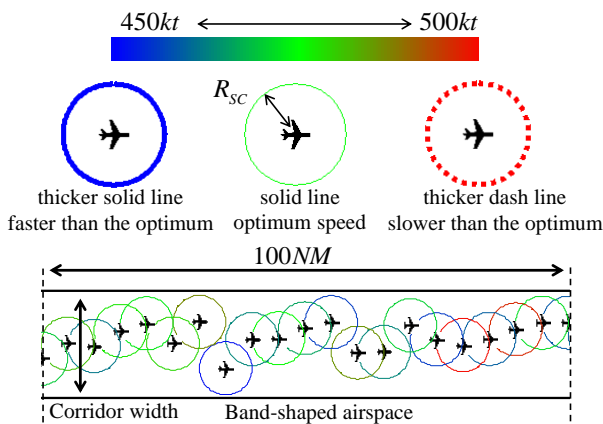


Fig. 10 Display example of traffic flow

3.2 Evaluation Indices

It is desirable that all the aircraft are able to fly at their optimum flight speed. However, to maintain the distance for safe operations, speed

control is required. Changing the speed affects the flight schedule and fuel efficiency. In this study, following index E_{vi} is introduced to roughly evaluate the effect of speed control:

$$E_{vi} = \int V_{oi} - V_i dt \quad (17)$$

where, V_{oi} is the optimum flight speed of aircraft i . It is also desirable for the feasibility of the self-separation algorithm that the control amount is as small as possible. The amount of the heading and speed change is calculated through numerical simulations as follows:

$$E_{whi} = \int \dot{\psi}_i dt \quad (18)$$

$$E_{wvi} = \int \dot{V}_i dt \quad (19)$$

To eliminate the influence of the initial conditions as possible, the evaluation indices are computed from 20,000 seconds after the start of the simulations.

3.3 Behavior of Aircraft in the Air Corridor

Examples of aircraft behavior under the developed algorithm are shown in Fig. 11. The snapshots of air traffic in the 3 corridors with different width are shown 18000 seconds and 36000 seconds after simulation start.

In the 10-NM-wide corridor, a deadlock occurred when the slower aircraft fly side by side. In high density traffic, aircraft catch up with preceding aircraft before they complete overtaking process. In the 20-NM-wide corridor, although many aircraft change their flight speed to avoid conflict, traffic flow without deadlock is realized. As the corridor width increases, aircraft could utilize more space to overtake. As a result, aircraft could fly at their optimum speed most of the simulation time.

3.4 Analysis

The evaluation indices are summarized in Fig. 12, 13. The value of E_v is extremely large in the 10-NM-wide corridor due to the deadlock. The relation between index of speed change and optimum flight speed in 5 typical cases with deadlock is shown in Fig. 14. In this algorithm,

**A SELF-SEPARATION ALGORITHM USING SPEED CONTROL
FOR WIDTH-LIMITED HIGH DENSITY AIR CORRIDOR**

each aircraft determines their flight speed based on approaching aircraft within a lateral distance of R_{SC} . Hence, the target speed of each aircraft for speed control is different in congested area.

Unless the overtaking process is finished swiftly, the distance becomes less than R_{SC} and the following aircraft reduce their speed for conflict avoidance. In this case, the following aircraft cannot increase their speed even though another following aircraft approaches. Additionally, since aircraft refers only current speed information, the preceding aircraft does not increase their speed when the following aircraft fly at the same speed as the preceding aircraft because conflict is not expected at the moment. As a result, the faster aircraft reduce their flight speed more than that of the slower aircraft. The values of E_{wh} and E_{wv} are small due to deadlock. In the 20-NM-wide corridor, since aircraft have some space to overtake, E_v is reduced and E_{wh} and E_{wv} are increased. As the corridor width increased, the indices are reduced because aircraft are self-separated only with small heading change.

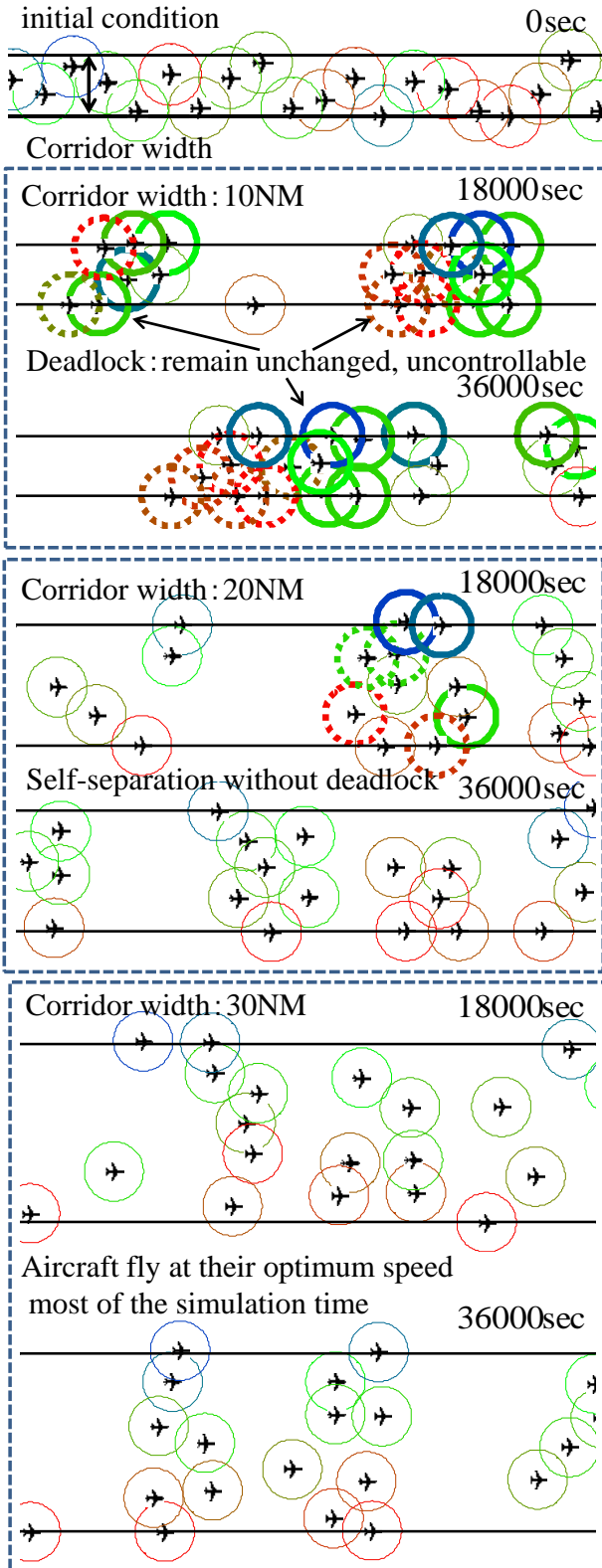


Fig. 11 Behavior of aircraft in the corridor with different width

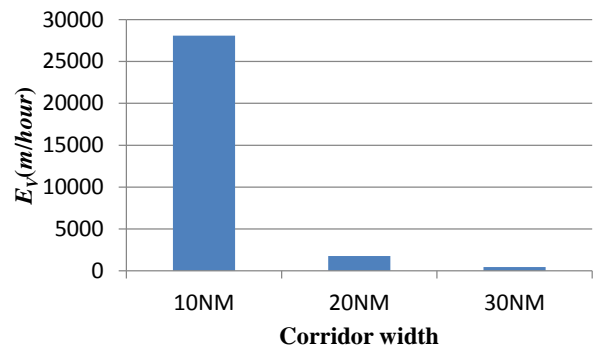


Fig. 12 Index of speed change

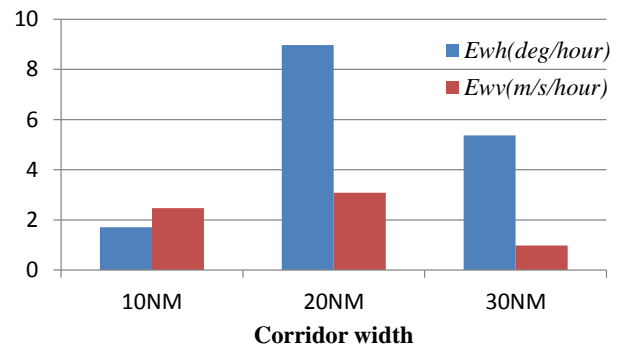


Fig. 13 Index of control amount

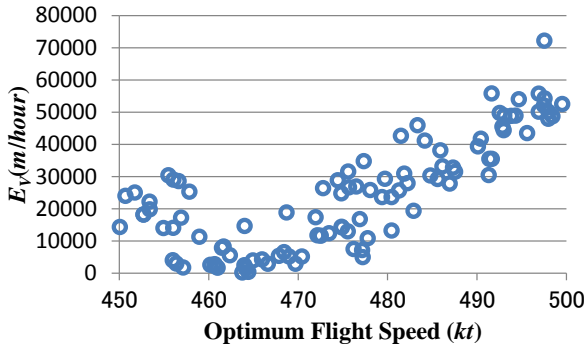


Fig. 14 Relation between E_v and optimum flight speed in 5 deadlock scenarios

3.5 Algorithm for Operational Improvement

The causes of the deadlock occurred in 10-NM-wide corridor are shown in Fig. 15. Aircraft got stuck as cause 1 in the Fig. 15 shows. In this case, aircraft could not overtake other aircraft with any maneuver. Even though lateral distance is maintained like the cause 2 in the Fig. 15, where aircraft A and B are flying at same speed V_{line}^1 , aircraft C and D are flying at V_{line}^3 , C is flying at V_{line}^2 , this situation results in the deadlock if these speeds are almost the same. It takes a long time for the aircraft to complete overtaking process with aircraft flying at similar speed. If other aircraft catch up with the group of aircraft with overtaking process unfinished, it is more difficult to complete overtaking and the congested situation result in the cause 1.

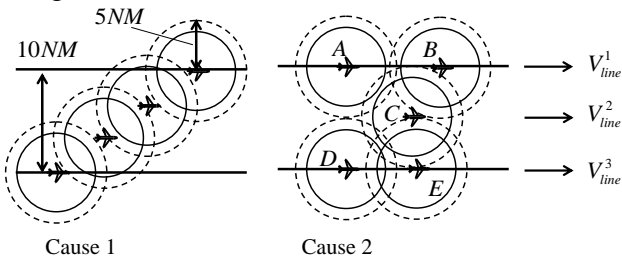


Fig. 15 Causes of the deadlock

To prevent a deadlock, sub-route is newly introduced in the corridor as shown in Fig. 16. Aircraft in the corridor are flying on the sub-route except for the changing sub-route to overtake another aircraft. An installation of sub route prevents aircraft from sticking as shown the cause 1 in Fig. 15. Furthermore, the information of optimum speed is considered. It is difficult to determine appropriate maneuver

for the aircraft under speed control only with current speed information. As shown in Fig. 11 and 14, it is indicated that the slower aircraft become a bottleneck and the aircraft with faster optimum speed reduce their speed. The algorithm including sub-route referring the optimum speed are developed and traffic calculated with the new algorithm is evaluated to examine the effect of operational improvement.

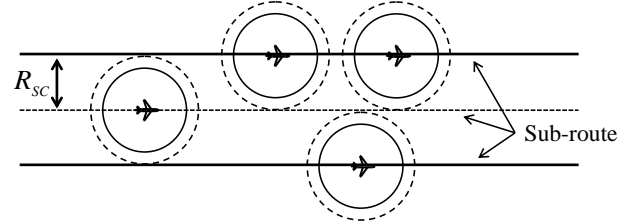


Fig. 16 Installation of sub-route

3.6 Operational Improvement Evaluation

Examples of aircraft behavior under the revised algorithms are shown in Fig. 17. In this simulation, aircraft are flying on the sub-route referring to the optimum speed information. As a result, in the 10-NM-wide corridor where deadlock occurred in the previous simulation, aircraft complete overtaking without deadlock. As the same way before, aircraft could fly at optimum flight speed most of the simulation time. The evaluation indices are calculated as shown in Fig. 18, 19. In the figures, the indices as mentioned before are compared. Original means traffic with self-separation algorithm using current information as 3.3 shows, and revised means the algorithm introduced sub-route and optimum speed. It is indicated that revised algorithm leads aircraft to fly on the sub-route and deadlock is resolved. Therefore, the value of speed control index in the 10-NM-wide corridor is reduced drastically. On the other hand, to complete overtaking in the narrow corridor, the control indices are increased. It is also indicated that the revised algorithm reduces the control index in the 20, 30-NM wide corridors. Designating route reduce the control amount required when aircraft adjust to overtake another aircraft, and utilization of optimum speed is useful to determine the aircraft to overtake. The relation between E_v and optimum flight speed in the

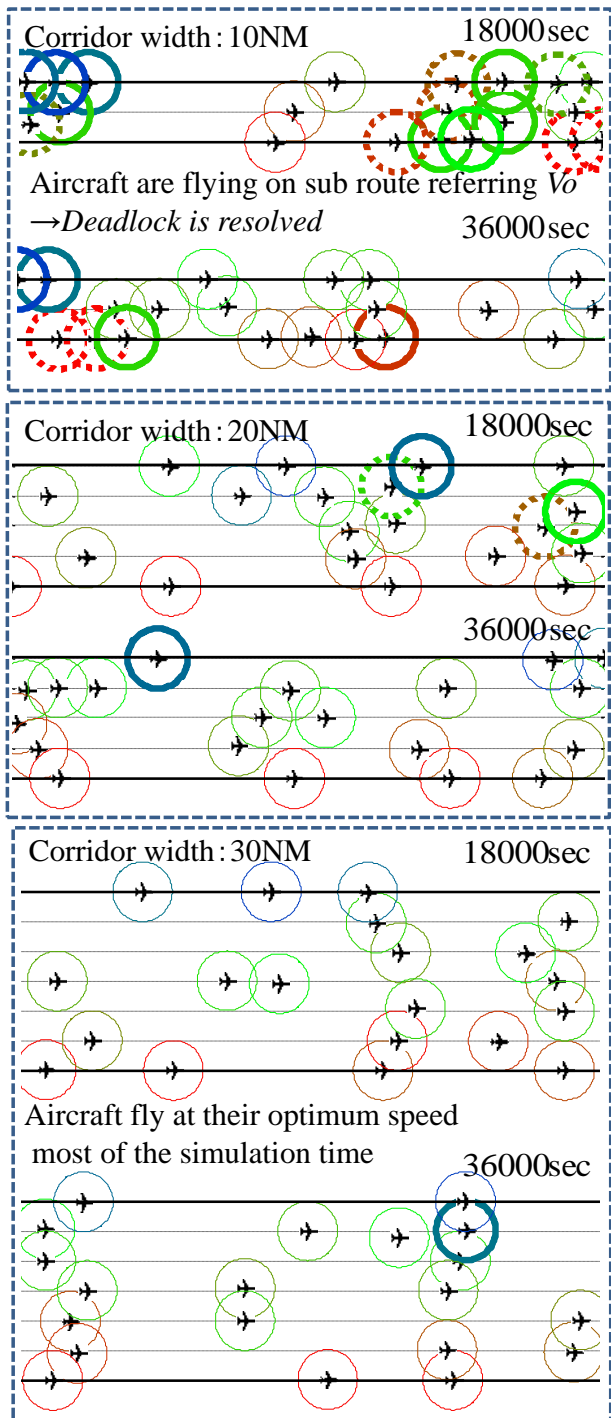


Fig. 17 Behavior of aircraft in the corridor with different width

same scenarios shown in Fig. 14 is also examined. The result is shown in Fig. 20. It is clarified that the utilization of sub-route and optimum flight speed information is able to reduce the inequities between aircraft with faster optimum speed and slower optimum speed.

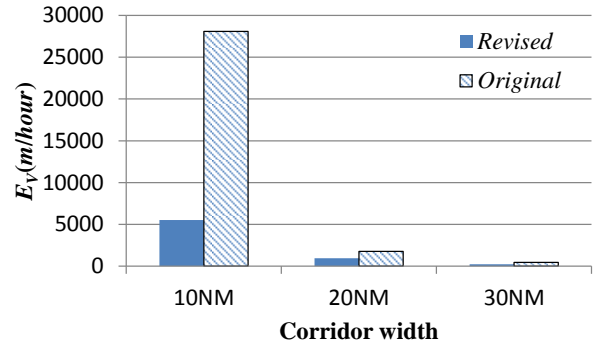


Fig. 18 Index of speed changed

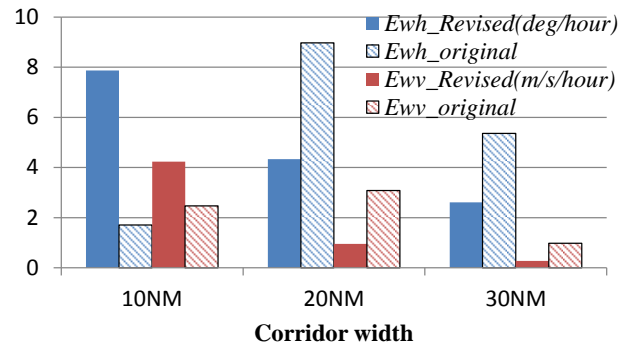


Fig. 19 Index of control amount

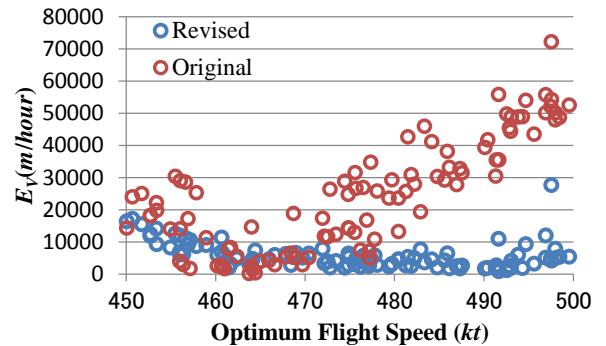


Fig. 20 Relation between E_v and optimum flight speed in the same scenarios as shown in Fig. 14

4 Conclusion

The aircraft self-separation algorithms for width-limited air corridor operation were discussed. Self-separation algorithm using heading and speed change has been developed and traffic flow without conflict was realized in the width-limited air corridor.

It was shown that the self-separation using current state information could result in a deadlock in the narrow air corridor. As the corridor width increased, aircraft utilized more

space and completed overtaking without deadlock. It was indicated that the installation of sub-route and utilization of optimum speed information prevented a deadlock and reduced inequities between aircraft with different optimum flight speed even though the corridor width is narrow.

To bring the air corridor operation into practical use, the relation between airspace resources and actual traffic volume should be investigated and the geometry of the corridor is also important to realize the conflict-free corridor operation without deadlock.

There are a lot of future works. The more practical procedures including altitude change should be investigated. Allocations of the air corridor are important issue for efficient implementation and emergency procedures are indispensable. In addition, the traffic flow should be evaluated from a more practical viewpoint such as fuel consumption, punctuality, etc.

References

- [1] Joint Planning and Development Office, "Concept of Operations for the Next Generation Air Transportation System Version," Version 3.2, Sep. 30, 2010.
- [2] Japan Civil Aviation Bureau, "Long-term Vision for the Future Air Traffic Systems (CARATS)," URL: http://www.mlit.go.jp/koku/koku_CARATS.html [cited June 15, 2013].
- [3] RTCA, DO-242a, "Minimum Aviation System performance standards for Automatic Dependent Surveillance Broadcast (ADS-B)," June 25, 2002.
- [4] Arash Yousefi, Jerome Lard, and John Timmerman, "NextGen Flow Corridors Initial Design, Procedures, and Display Functionalities," IEEE/AIAA 29th Digital Avionics System Conference, Oct. 3-7, 2010.
- [5] Arash Yousefi, Ali N. Zadeh, and Ali Tafazzoli, "Dynamic Allocation and Benefit Assessment of NextGen Flow Corridors," 10th AIAA ATIO Conference, Fort Worth, Texas, 2010.
- [6] Xue, M, "Design Analysis of Corridors-in-the-sky," AIAA Guidance, Navigation, and Control Conference, Chicago, Aug. 10-13, 2009.
- [7] Nakamura, Y. and Takeichi, N., "Unidirectional Air Traffic Flow Control Using Airborne Surveillance," Journal of the Japan Society for Aeronautical and Space Sciences, Vol. 59, 2011, pp. 76-82 (in Japanese).
- [8] Nakamura, Y. and Takeichi, N., "Decentralized Control of an Unidirectional Air Traffic Flow with Flight Speed Distribution," Journal of the Japan Society for Aeronautical and Space Sciences, Vol. 60, 2012, pp. 17-23 (in Japanese).
- [9] Takeichi, N., Nakamura, Y., Fukuoka, K. "Fundamental Characteristics of Decentralized Air Traffic Flow Control in High Density Corridor," 28th International Congress of the Aeronautical Sciences, 2012.
- [10] Takeichi, N., Nakamura, Y., Kageyama, K., "Aircraft Self-Separation Algorithm for High Density Corridor Operation Based on Flight Intent," Transactions of the Japan Society for Aeronautical and Space Sciences, Vol. 57, No. 3, May 2014, pp.179-185.
- [11] Nakamura, Y., Takeichi, N. and Kageyama, K., "A Self-Separation Algorithm using Relative Speed for High Density Air Corridor," AIAA-2013-5069, AIAA Modeling and Simulation Technologies Conference, Boston, Aug. 19-22, 2013.

Contact Author Email Address

y-nakamura@enri.go.jp

Copyright Statement

The authors confirm that they, and/or their company or organization, hold copyright on all of the original material included in this paper. The authors also confirm that they have obtained permission, from the copyright holder of any third party material included in this paper, to publish it as part of their paper. The authors confirm that they give permission, or have obtained permission from the copyright holder of this paper, for the publication and distribution of this paper as part of the ICAS 2014 proceedings or as individual off-prints from the proceedings.